

BEAM LOSS MEASUREMENTS DURING INJECTION INTO THE ADVANCED PHOTON SOURCE UPGRADE STORAGE RING*

J. Dooling[†], A. Brill, J. Calvey, W. Cheng, V. Sajaev, Argonne National Laboratory, Lemont, USA

Abstract

A fiber-optic (FO) beam loss monitor (BLM) system, installed along the booster to storage ring (BTS) transport line has been useful in identifying loss locations employing time-of-flight (TOF) analysis. The BTS BLM TOF system is comprised of a pair of rad-hard, fused-silica FO cables running along either side of the BTS line at beam elevation. In the initial configuration, we measured losses at both the upstream (US) and downstream (DS) ends of the FO cable pair. However, losses further DS along the septum and injection kicker set are also of interest. We therefore added a 20-m-length, multi-strand fused-silica FO cable bundle, replacing the DS outer FO radiator input. Thus, three of the detectors are configured at the US end of their respective FO radiators. The US detector location provides lower signal but improved spatial resolution over the DS. Loss location identification has been accomplished by inserting YAG screen flags at different positions along the BTS. We present results from studies and operations.

INTRODUCTION

We previously described a fiber-optic (FO) time-of-flight (TOF) fast beam loss monitor (BLM) system installed in the booster-to-storage ring (BTS) transport line at the Advanced Photon Source (APS) [1]. This system was recently modified to allow a 20-m length of fiber radiator to extend from the downstream (DS) photomultiplier tube (PMT) detector location further downstream to just beyond the S40 horizontal collimator. The DS detectors are located under the DQ2 magnet (Fig. 1). The upstream (US) detectors are located under the AQ1 magnet just after the booster extraction kickers (Fig. 1, top). Both detector locations are Pb-shielded. The installation of the new FO cable was done during the January 2025 maintenance period. Initially, the downstream end of this fiber bundle was pulled just past the swap-out dump in the S40 A:M1 dipole magnet. This arrangement left approximately 2 meters of slack at the US end of the cable. During the May 2025 maintenance period, the slack was removed and the FO cable end was pulled an additional 2-m further downstream. This FO cable now extends downstream of the injection septum and kickers as well as past the swap-out dump and the S40 horizontal collimator locations.

ANALYSIS

Several challenges must be overcome in order to determine loss position. First, beam loss will shower downstream from its strike location. Second, the speed at which light travels

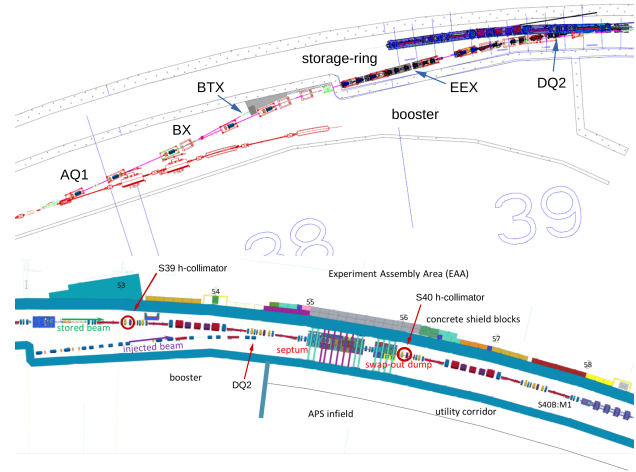


Figure 1: The booster to storage-ring (BTS) transport line. Top: The US PMT detectors are located under the AQ1 magnet, and the downstream detectors under the DQ2 magnet. Both are locations are Pb-shielded. Bottom: The added FO cable radiator now extends downstream past the S40 h-collimator location.

in the fused silica fiber used here is wavelength dependent. The fiber index of refraction, n_f can be determined using Malitson's expression [2] for a given wavelength between 210 and 3710 nm. Čerenkov radiation is relatively broadband; however it does favor the blue end of the spectrum. The Hamamatsu R7400U-06 subminiature photomultiplier tube (PMT) employed here to convert light to electrical signals has an extended UV range [3]. The cathode radiant sensitivity is near 20 mA/W at 200 nm, rising to 34 mA/W at 260 nm.

Prior to saturation, gain as a function of bias voltage, V for this PMT family is expressed as [4],

$$G(V) = G_o \left(\frac{V}{V_o} \right)^{N_d - 1}, \quad (1)$$

where $G_o = 5 \times 10^5$ at $V_o = 800$ V and N_d is the number of dynodes; here $N_d = 8$.

The PMT signals from each of the four channels are recorded on a 2.5-GHz bandwidth Teledyne-Lecroy Model 9254M oscilloscope. The time signals can be mapped into spatial positions, s_u and s_d along the BTS line using a simple model presented in Eqs. (2) and (3), respectively [5].

$$s_u(t) = \frac{c(t - t_{ref,u})}{n_f + 1}, \quad (2)$$

$$s_d(t) = -\frac{c(t - t_{ref,d})}{n_f - 1}, \quad (3)$$

* Work supported by the U.S. D.O.E., Office of Science, Office of Basic Energy Sciences, under contract number DE-AC02-06CH11357.

[†] dooling@anl.gov

n_f is the fiber index of refraction, c is the vacuum speed of light, and t_{ref} is the reference time delay for US or DS channels. The TOF analysis assumes a single refractive index ignoring chromatic effects. Čerenkov radiation tends towards the blue end of the spectrum but is not monochromatic. From Eqs. (2) and (3), the minimum resolvable Δs are $\Delta s_{u,min} = c\Delta t_{min}/(n_f + 1)$ and $\Delta s_{d,min} = c\Delta t_{min}/(n_f - 1)$. Assuming $\Delta t_{min} \approx 1$ ns and $n_f = 1.5$, $\Delta s_{u,min} = 0.12$ m and $\Delta s_{d,min} = 0.60$ m. However when attempting to use n_f values as high as 1.538 ($\lambda = 210$ nm), mapped locations would extend beyond the physical length of the fiber. An index of 1.700 provided the required spatial limit.

MEASUREMENTS

Insertion of BTS YAG Screens

Waveforms were recorded in April 2025 while inserting BTS YAG screens [6] with 1 nC extracted from the booster and minimum applied bias on all the PMTs (−400 V, Fig. 2). Just prior to the BTS YAG screen study, beam was being directed to the BTX dump using the BX dipole (Fig. 1). Optimization of extracted booster beam had not yet been completed and significant losses were occurring near the booster extraction septum and kickers (Fig. 3). Bias levels

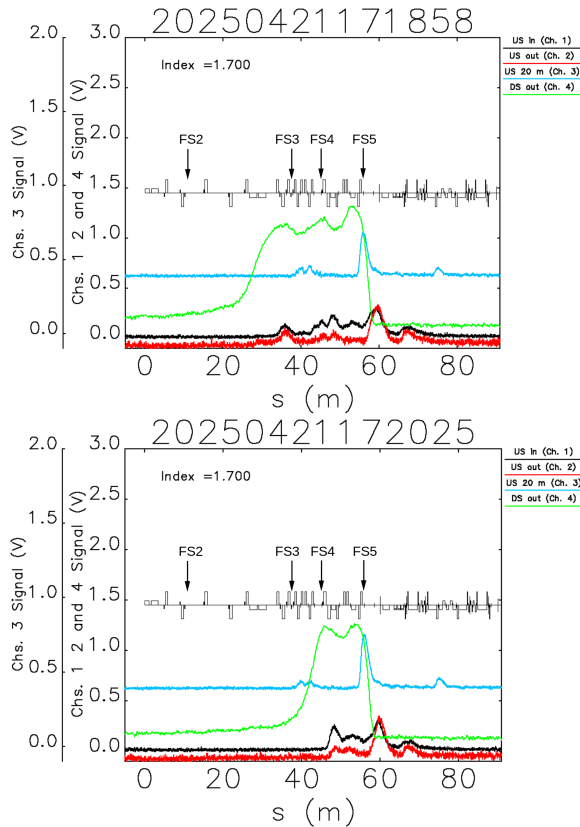


Figure 2: Loss monitor waveforms using time-of-flight analysis to map time signals in spatial locations, s along the BTS line. For channels 1, 2, and 3, positions are determined from Eq. (2) and for ch. 4, Eq. (3). Top: FS3 in and bottom: FS4 in.

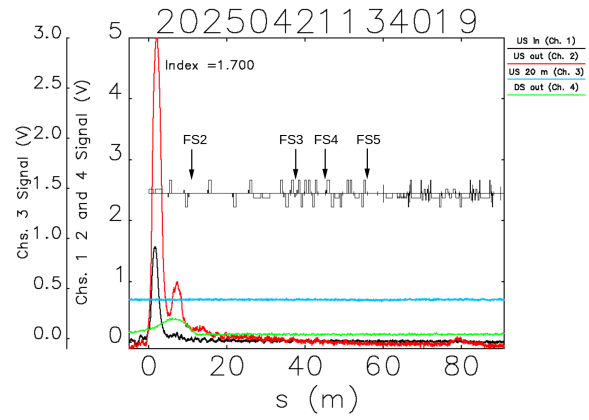


Figure 3: BTS BLM waveforms prior to booster extraction optimization and the flag insertion study. BX dipole on.

here for US channels 1 and 2 were higher: −900 V, and on Ch. 4: −500 V. Losses are seen at the far US end of the booster/Zone F fibers and nothing is observed on the injection DS fiber due to beam being directed to the BTX dump. Though the US outer fiber (Ch. 2) shows a large signal, the gain based on Eq. (1) is 290 times greater for Chs. 1 and 2 than during the flag test, and 4.8 times greater for Ch. 4. The gain on Ch. 3 was unchanged.

Injection Without Swap-Out

Initially the signal on the injection fiber (Ch. 3) was assumed to be a combination of both injection and swap-out losses; however, this turned out not to be the case. A study was conducted where a single bunch would be injected into an empty SR and then blocked with a horizontal collimator in S01. An orbit bump was installed to insure the beam would strike the collimator so that only injection losses would be seen on Ch. 3; however, none were observed. Only when swap-out was enabled were signals present on the downstream injection fiber (Fig. 4).

Operations

Losses in the BTS line vary considerably over the course of a run. After optimizing low-charge injection, signals on the fibers upstream of DQ2 can fall below the noise level. Losses during high-charge, timing-mode operation tend to be larger. During the last two weeks of User Run 2025-2 (23 July-5 August), output charge data from the Ch. 4 detector was compared with injection efficiency, η_{inj} (Fig. 5). PMT charge initially drops as η_{inj} increases as one might expect, but then becomes noisy at higher efficiencies. The noise may be due to optimization that was taking place when the BTS BLM data was collected. The HV bias for these measurements was set at either −800 and −900 V; thus based on Eq. (1), the charge extracted from the PMT photocathode was on the order of 1 fC.

Radiation Monitor

After the 2025-1 and 2025-2 User Runs, Health Physics did radiation surveys along the BTS line. Count rates along

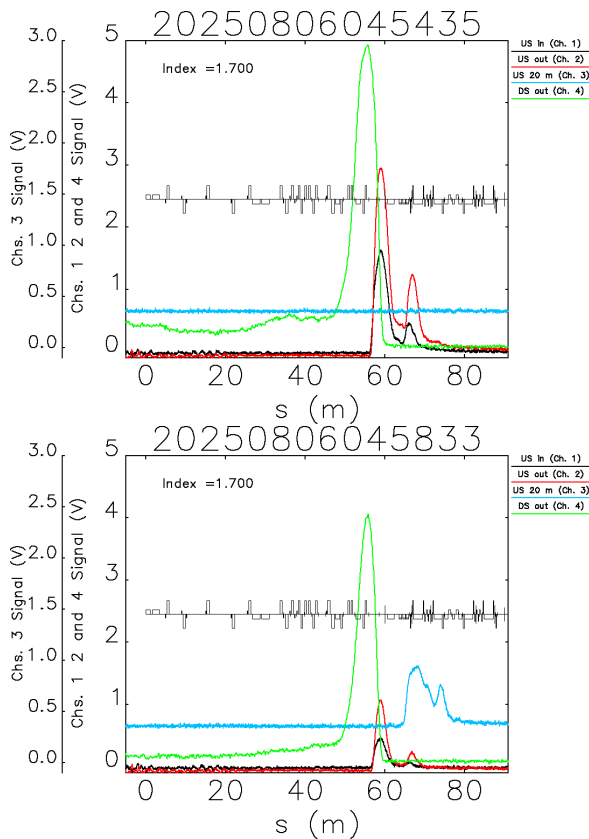


Figure 4: Mapped loss signals with a single 13-nC bunch injected into the SR. Top: Path blocked with beam bump. Bottom: Bump removed with swap-out enabled.

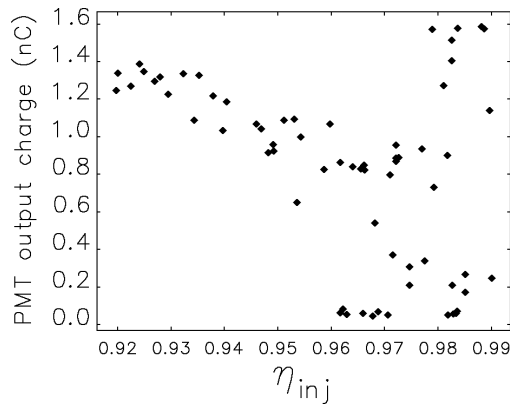


Figure 5: Injection efficiency of the charge injected into the APS-U SR vs. Ch. 4 PMT output charge.

the BTS from the AQ1 to the DQ2 were measured using a Ludlum Model 3000 Gamma Detector (Fig. 6). The large activity seen near the DQ1 magnet is consistent with BTS BLM signals recorded near the end of User operations.

DISCUSSION AND SUMMARY

The newly installed FO radiator is not as sensitive to loss in the BTS due to its placement away from the beam line; however, the large signal amplitudes observed from swap-out indicate the wide range of intensities that must be covered.

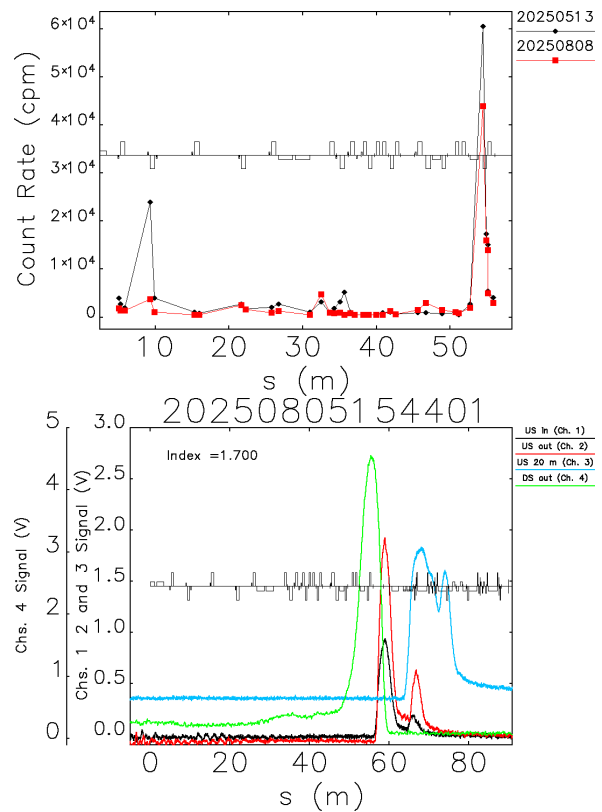


Figure 6: Top: Radiation count rates measured along the BTS line from AQ1 to DQ2. Bottom: BTS BLM signals recorded during timing mode operation near the end of the 2025-2 User Run.

Signals from s-distributed losses in the US detectors reflect the forward direction in time and are expanded temporally. On the other hand, the DS detectors see a spatial distribution reversed in time and compressed. If losses are concentrated at a single spatial position along the FO, both US and DS detectors will see a forward-time loss signal, still stretched or compressed as before; however, the signal waveform temporal profile will be that of the bunch profile. RMS bunch duration in the APS booster at extraction is measured to be approximately 100 ps [7]; whereas, the risetime of the PMT is given as 780 ps. Thus the bunch duration from a single loss point cannot be resolved.

In summary, the BTS FO-based BLM provides loss location information and shows the effects of the resulting electromagnetic shower. We are puzzled by the necessity to increase the index of refraction over expected values in order to limit the loss locations to the physical length of the FO along the BTS. Because of the high sensitivity and large dynamic range of loss intensity, calibrating loss signals to actual lost charges is challenging.

ACKNOWLEDGMENTS

Thanks to J. Lie and B. Micklich for supplying Fig. 1. Thanks also to R. Soliday and H. Shang for assistance with analysis scripts.

REFERENCES

- [1] J. Dooling, A. Brill, J. Liu, S. Shoaf, and S. Wang, “Time-of-flight beam loss monitor for the Advanced Photon Source Upgrade booster-to-storage-ring transport line”, in *Proc. IPAC’24*, Nashville, TN, USA, May 2024, pp. 3348–3351. doi:10.18429/JACoW-IPAC2024-THPG40
- [2] I. H. Malitson, “Interspecimen comparison of the refractive index of fused silica”, *J. Opt. Soc. Am.*, vol. 55, no. 10, pp. 1205–1209, Oct. 1965. doi:10.1364/JOSA.55.001205
- [3] *Metal package photomultiplier tube R7400U series*, Hamamatsu. https://ctf3-tbts.web.cern.ch/instr/PMT/R7400U_TPMH1204E07.pdf
- [4] J. C. Dooling, M. Borland, K. C. Harkay, R. T. Keane, B. J. Micklich, and C. Yao, “A Fast Beam Interlock System for the Advanced Photon Source Particle Accumulator Ring”, in *Proc. IPAC’18*, Vancouver, Canada, Apr.–May 2018, pp. 1815–1818. doi:10.18429/JACoW-IPAC2018-WEPAF005
- [5] A. Fisher *et al.*, “Beam-loss detection for the high-rate superconducting upgrade to the SLAC linac coherent light source”, *Phys. Rev. Accel. Beams*, vol. 23, no. 8, p. 082802, 2020. doi:10.1103/PhysRevAccelBeams.23.082802
- [6] K. P. Wootton and A. H. Lumpkin, “Sublinear intensity response of cerium-doped yttrium aluminium garnet screen with charge”, in *Proc. NAPAC’22*, Albuquerque, NM, USA, Aug. 2022, pp. 437–440. doi:10.18429/JACoW-NAPAC2022-TUPA38
- [7] J. Dooling, J. Calvey, and O. Mohsen, “Bunch duration measurements in the APS-U booster”, presented at NAPAC’25, Sacramento, CA, USA, Aug. 2025, unpublished.